JACS
JOURNAL OF THE AMERICAN CHEMICAL SOCIETY
Article
pubs.acs.org/JACS

Methane Reacts with Heteropolyacids Chemisorbed on Silica to Produce Acetic Acid under Soft Conditions

Miao Sun,[†] Edy Abou-Hamad,[†] Aaron J. Rossini,[‡] Jizhe Zhang,[§] Anne Lesage,[‡] Haibo Zhu,[†] Jeremie Pelletier,[†] Lyndon Emsley,*[,‡] Valerie Caps,*[,†,⊥] and Jean-Marie Basset*[,†]

[†]KAUST Catalysis Center and [§]Division of Chemical and Life Sciences and Engineering, King Abdullah University of Science and Technology, Thuwal, 23955-6900, Saudi Arabia

[‡]Université de Lyon, (CNRS/ENS-Lyon/UCB Lyon 1), Centre de RMN à Très Hauts Champs, 5 rue de la Doua, 69100 Villeurbanne, France

Supporting Information

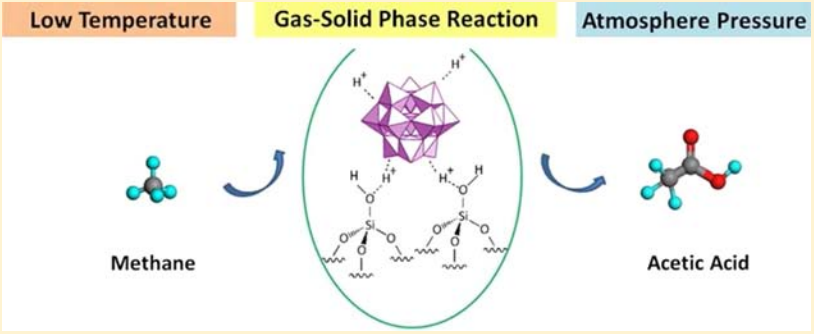

ABSTRACT: Selective functionalization of methane at moderate temperature is of crucial economic, environmental, and scientific importance. Here, we report that methane reacts with heteropolyacids (HPAs) chemisorbed on silica to produce acetic acid under soft conditions. Specially, when chemisorbed on silica, $H_4SiW_{12}O_{40}$, $H_3PW_{12}O_{40}$, $H_4SiMo_{12}O_{40}$, and $H_3PMo_{12}O_{40}$ activate the primary C−H bond of methane at room temperature and atmospheric pressure. With these systems, acetic acid is produced directly from methane, in a single step, *in the absence of Pd and without adding CO*. Extensive surface characterization by solid-state NMR spectroscopy, IR spectroscopy, cyclic voltammetry, and X-ray photoelectron spectroscopy suggests that C−H activation of methane is triggered by the protons in the HPA−silica interface with concerted reduction of the Keggin cage, leading to water formation and hydration of the interface. This is the simplest and mildest way reported to date to functionalize methane.

INTRODUCTION

Selective functionalization of methane at moderate temperature is of crucial economic importance due to the low cost and high abundance (methane accounts for up to 90% of natural gas) of this compound.[1] Its chemistry also presents a major scientific challenge, since activation of the primary C−H bond of methane is energetically highly demanding (440 kJ/mol).[2] Several modes of low temperature activation/functionalization have already been proposed,[3] typically involving either electrophilic activation (by superacids) or oxidative addition (on group VIII metals) in sophisticated homogeneous systems operated at high pressure.[4−15]

Direct and unexpected conversion of methane to acetic acid was observed by Periana et al. with a system. The system consists of Pd^{II} in fuming sulfuric acid, which behaves as an oxidant, and operates at 30 atm/180 °C. It leads to CH_3COOH (after hydrolysis of the main CH_3COOSO_3H product) and CH_3OH.[16] The catalytic reaction was suggested to occur by carbonylation of a Pd−CH_3 species resulting from the C−H bond activation of methane by a simple electrophilic substitution mechanism.[7,12] CO is generated in situ from the slow overoxidation of the methanol intermediate, and no reaction was observed in the absence of Pd. The catalyst was reported to yield modest turnover numbers (5−18) after several hours of reaction before losing its activity. The Pt version of this system, which leads to methanol, also undergoes deactivation in a matter of hours, due to product and water inhibition.[17] The efficiency of these systems seems to rely on the strength of the acidic medium; a concentration of sulfuric acid above 96% is required.[18] Recently, a cocatalytic effect of the strongly acidic reaction medium in the Catalytica−Periana system was reported.[19]

Liquid superacids (such as HF−SbF_5) are also known to directly activate methane at low temperature. This unexpected reactivity, initially developed by Olah, was attributed to a CH_3^+ carbonium species resulting from protolytic cleavage of the methane C−H bond, followed by hydrogen abstraction. It

Received: October 9, 2012
Published: December 26, 2012

dx.doi.org/10.1021/ja309966j | J. Am. Chem. Soc. 2013, 135, 804−810

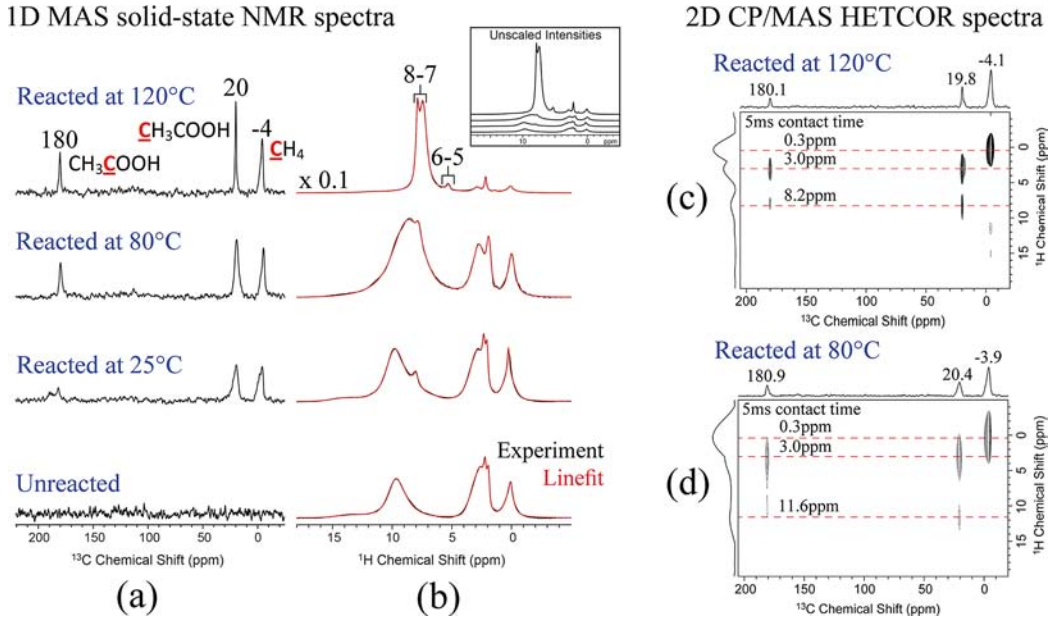

Figure 1. One-dimensional (1D) MAS solid-state NMR spectra: ^{13}C CP/MAS solid-state NMR spectra (a) and 1D ^{1}H MAS NMR spectra (b) of $H_4SiW_{12}O_{40}/SiO_{2\text{-}(500)}$ samples before and after reaction with $^{13}CH_4$ at 25, 80, and 120 °C. 2D CP/MAS HETCOR spectra of $H_4SiW_{12}O_{40}/SiO_{2\text{-}(500)}$ samples obtained after reaction with $^{13}CH_4$ at 120 °C (c) and 80 °C (d). All spectra were acquired at room temperature. Both 2D CP/MAS HETCOR spectra were acquired with long contact times (5 ms) in order to probe for contact between carbon and nonbonded protons. Details of the ^{1}H MAS NMR line fitting are given in the Supporting Information. Note that the intensity of the ^{1}H MAS NMR spectrum of 120 °C reacted material has been scaled by a factor 0.1 due to large increase in the number of protons in the material upon reaction (see the text for details).

leads, at about 140 °C[4] to polycondensation products (mostly the trimethylcarbonium ion, dimethylisopropylcarbonium ion, and higher molecular weight hydrocarbon ions) and hydrogen.[5] In the presence of CO, superacids such as $FHSO_3-SbF_5$ allow direct carbonylation of methane (50 atm) from 60 °C.[20−22]

The latest approaches focus on the metal center of homogeneous/soluble counterparts/analogues to design molecular-inspired solid reagents for clean methane-to-methanol transformation.[23−25] Considering the role of the acidic part of the Catalytica−Periana system, here, we evaluate the potential of solid acids in the methane to acetic acid transformation. Solid acids, such as the tungsto−silicic heteropolyacid (HPA) with Keggin structure, $H_4SiW_{12}O_{40}$, are indeed being used at the industrial level (Showa−Denko process) for direct ethyl acetate production from ethylene.[26] At the molecular level, this transformation is thought to involve a Wacker-type mechanism, in which activation of the vinylic carbon−hydrogen bond occurs on the Pd^{2+} component of the silica-supported catalyst. In this model, the HPA is proposed to act essentially as a cocatalyst by regenerating the active Pd site, and in the absence of Pd, the supported HPA is reported to be inactive for the formation of acetic acid.[27] However, low yields of acetic acid can be obtained directly from ethane on Pd-free supported molybdo(vanado)phosphoric HPAs,[28] suggesting that supported HPAs can activate secondary aliphatic C−H bonds (and the formation of secondary C−O bond), even in the absence of Pd.

Here, we report that methane reacts stoichiometrically with heteropolyacids chemisorbed on silica to produce acetic acid at mild temperatures and atmospheric pressure. Specially, when chemisorbed on silica, $H_4SiW_{12}O_{40}$, $H_3PW_{12}O_{40}$, $H_4SiMo_{12}O_{40}$, and $H_3PMo_{12}O_{40}$ activate the primary C−H bond of methane. With these systems, acetic acid is produced directly from methane, in a single step, *in the absence of Pd and without adding CO*. In this system, acetic acid is the only observed hydrogen-containing carbonaceous molecule produced on the material surface before appearing in the gas phase. This noble-metal-free heterogeneous gas−solid system operated in a fixed-bed flow reactor (residence time ∼12 s) is by far the simplest and mildest way reported so far to functionalize methane. We demonstrate that both C atoms of acetic acid are derived from methane. Notably, when exposed to methane, HPAs alone do not produce acetic acid; only HPA chemisorbed on dehydroxylated silica allows this transformation.

RESULTS AND DISCUSSION

The ^{13}C cross-polarization magic angle spinning (CP/MAS) NMR spectrum (Figure 1a) of $H_4SiW_{12}O_{40}/SiO_{2\text{-}(500)}$[29] in contact with flowing $^{13}CH_4$ (10% ^{13}C labeled, 5 mL/min, fixed-bed flow reactor) for 30 min at room temperature (25 °C) exhibits ^{13}C chemical shifts at 19.3 ppm ($-CH_3$) and 180.9 ppm ($-COO$). These chemical shifts are characteristic of acetic acid that has been physically adsorbed on oxide surfaces.[30] An additional resonance at approximately −4 ppm is attributed to physisorbed $^{13}CH_4$.[16,30,31] As the reaction temperature rises, from 25 to 80 °C, the intensity of both resonances increases. At 120 °C, the lines are narrower, but the integrated intensity is slightly less.

The two-dimensional (2D) CP/MAS $^{1}H-^{13}C$ heteronuclear correlation (HETCOR) spectra (contact time 0.4 ms) obtained at room temperature for a sample after reaction at 120 °C displays a correlation between the carbon signal at 19.8 ppm ($-CH_3$) and a proton signal at 3.0 ppm ($-CH_3$) and a correlation between the carbon signal at 180.1 ppm ($-COOH$) and a proton signal at 8.2 ppm ($-COOH$) (Figure S1, Supporting Information). In the CP/MAS HETCOR spectra acquired with a longer contact time (5 ms) obtained on samples treated at 80 °C (Figure 1d) and 120 °C (Figure 1c), the ^{1}H signals at 3.0 ppm ($-CH_3$) also correlate with the ^{13}C

dx.doi.org/10.1021/ja309966j | J. Am. Chem. Soc. 2013, 135, 804−810

signals at approximately 180 ppm (−COO), consistent with the fact that the $-CH_3$ and −COO functions belong to the same molecule (vide infra). These values slightly deviate from the chemical shifts of acetic acid dissolved in $CDCl_3$ (C: 178 and 20.3 ppm; H: 11.4 and 2.1 ppm),[32] likely due to the interaction between acetic acid and the silica support.

Interestingly, acetic acid is produced selectively on the surface, and no gaseous product is observed by gas chromatography (GC, with thermal conductivity detector), at least until the reaction temperature reaches 100 °C (Figure 2).

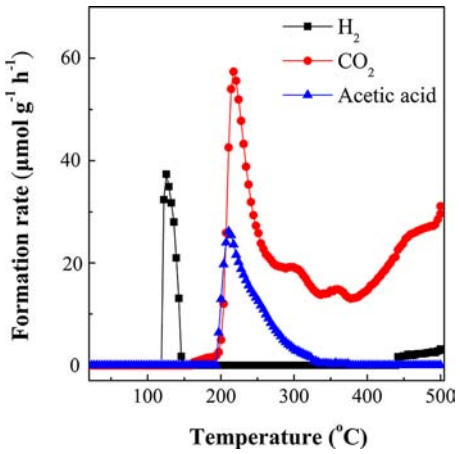

Figure 2. Product evolution during temperature-programmed activation of methane on $H_4SiW_{12}O_{40}/SiO_{2\text{-}(500)}$. Reaction conditions: $H_4SiW_{12}O_{40}/SiO_{2\text{-}(500)}$, 0.25 g; temperature raising rate, 50 °C h^{-1}; CH_4 flow rate, 5 mL min^{-1}.

All the chromatograms recorded below 100 °C are indeed free of any extra peak, except that of CH_4. Hence, no CO, CO_2, alkane, alkene, or oxygenated products other than acetic acid are formed, whether on the solid or in the gas phase, when CH_4 reacts with silica-supported HPA below 100 °C.

Under those conditions, the formation of acetic acid implies a reaction between methane and oxygens atoms of the chemisorbed HPA, according to the following stoichiometric equation:

$$2CH_4 + [H_4SiW_{12}O_{40}]/\text{silica} \rightarrow CH_3COOH + [H_4SiW_{12}O_{36}]/\text{silica} + 2H_2O$$

Indeed, in the course of this reaction, we observe that the interaction between HPAs and silica undergoes significant changes that can be followed by ^{1}H MAS solid-state NMR (Figure 1b). Before the reaction with methane, the ^{1}H MAS solid-state NMR spectrum of $H_4SiW_{12}O_{40}/SiO_{2\text{-}(500)}$ after line fitting exhibits three groups of intense resonances with chemical shifts of 1.8, from 2.6 to 3.0, and 9.7 ppm (Figure S2, Supporting Information). These correspond, respectively, to unreacted isolated silanols [≡Si—OH],[33] protonated silanols $[\equiv Si—O(H)_2]^+[HPA]^-$,[34] and HPA protons with limited interaction with the surface but likely interacting with [W]═O.[35] The peak at 1.8 ppm is already observed in the ^{1}H MAS NMR spectrum of $SiO_{2\text{-}(500)}$ before HPA deposition (Figure S3, Supporting Information). This demonstrates that, upon grafting, some silanols of the silica have not reacted with HPA. The broad peak at approximately 9.7 ppm is observed in the ^{1}H MAS NMR spectrum of unsupported, dehydrated $H_4SiW_{12}O_{40}$ (Figure S4, Supporting Information); it likely corresponds to the protons of the physisorbed HPA that are free from any interaction with the silica. Note the peak at 0 ppm is assigned to grease and/or physisorbed methane.

The ^{1}H NMR peaks between 2.6 and 3.0 ppm, which are absent from the spectrum of $SiO_{2\text{-}(500)}$ or the spectrum of dehydrated $H_4SiW_{12}O_{40}$, therefore result from the interaction between $H_4SiW_{12}O_{40}$ and the silica surface. This chemical shift range is consistent with protonated silanol groups $[\equiv Si—O(H)_2]^+$ (Figure 3A).

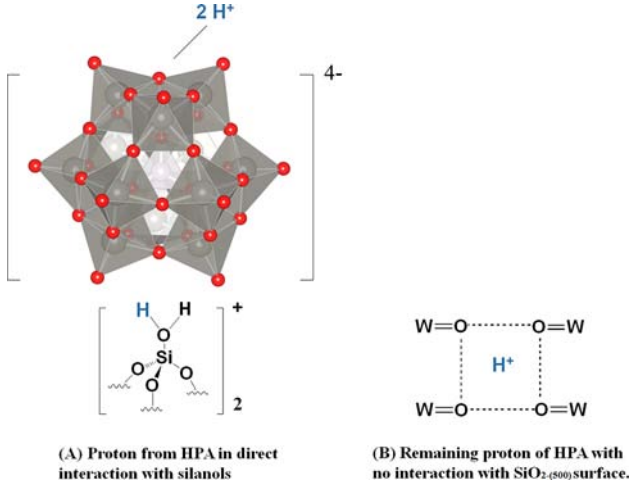

Figure 3. Proton species in the $H_4SiW_{12}O_{40}/SiO_{2\text{-}(500)}$ sample: (A) proton from HPA in direct interaction with silanols; (B) remaining proton of HPA with no interaction with the $SiO_{2\text{-}(500)}$ surface.[35]

This interpretation is further evidenced by strong autocorrelation peaks in double-quantum (DQ) and triple-quantum (TQ) ^{1}H−^{1}H dipolar correlation NMR spectra (Figure 4).[36−39] The intense autocorrelations indicate that protons of this type are densely clustered in groups of three or more at the HPA/silica interface. In the DQ spectrum, the protonated silanols are also observed to correlate with HPA acid protons at approximately 9.7 ppm (correlation at 11−14 ppm in the indirect DQ dimension). This indicates a close spatial proximity between the noninteracting acid protons and silanols that are hydrogen bonded to the HPA. On the other hand, an autocorrelation of the signal at approximately 9.7 ppm is observed only in the DQ spectrum and is absent from the TQ spectrum, which suggests that these protons do not belong to H_3O^+ or $H_5O_2^+$. These acid protons likely interact with the more accessible terminal oxygen of four HPA units, that is, [W]═O···H$^+$···O═[W] (Figure 3B).[35] This suggests that, when the HPA is sorbed on the silica surface, two (or one) protons remain free from the interaction with the silica surface and that the other two (or three) are likely involved in the interaction with surface silanols (Figure 3A). (We note in passing that the DQ spectrum recorded on the sample reacted at 80 °C also confirms the presence of acetic acid through correlations between CH_3 at 3 ppm and COO*H* protons at 11.9 ppm (Figure 4).)

As $H_4SiW_{12}O_{40}/SiO_{2\text{-}(500)}$ contacts the flowing $^{13}CH_4$ (10% ^{13}C labeled, 5 mL/min, fixed-bed flow reactor) with increasing temperature, the peak at approximately 2.6 ppm in the proton NMR spectrum gradually decreases in integrated intensity while the peak at 9.7 ppm disappears (Figure S2, Supporting Information). On the other hand, after reaction at 120 °C, two new signals appear: a weak sharp signal in the range 5−6

dx.doi.org/10.1021/ja309966j | J. Am. Chem. Soc. 2013, 135, 804−810

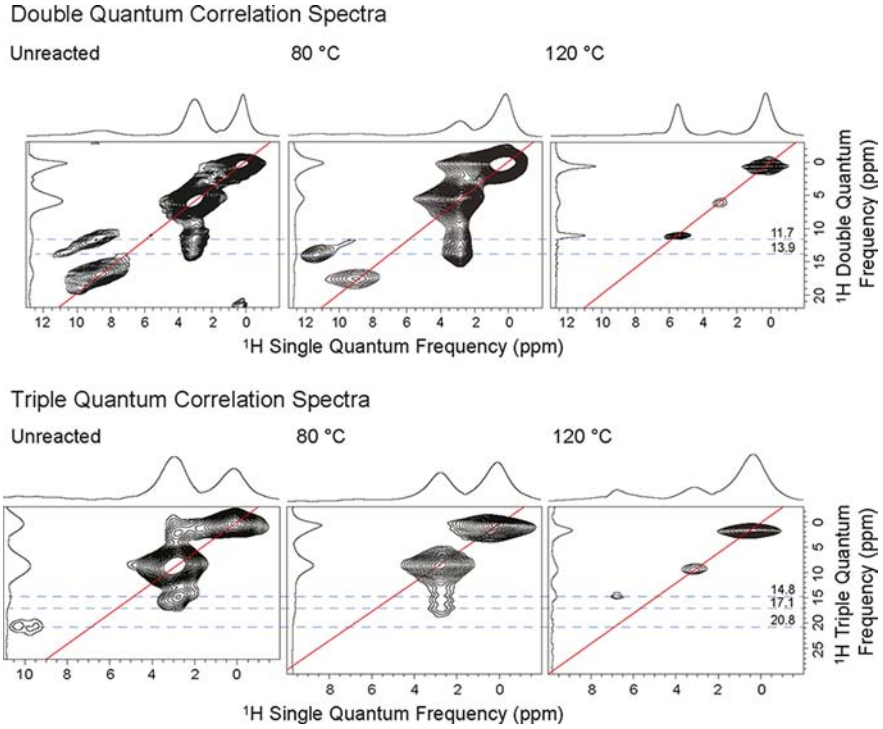

Figure 4. DQ and TQ ^{1}H–^{1}H NMR spectra of $H_4SiW_{12}O_{40}/SiO_{2\text{-}(500)}$ samples obtained before and after reaction with CH_4 at 80 and 120 °C. Spectra of the unreacted material were acquired on an 800 MHz spectrometer, while the other spectra were acquired on a 500 MHz spectrometer (see the Experimental Section for details). All spectra were acquired at room temperature.

ppm and an intense one in the range 7–8 ppm (Figure 1b). These signals are the main resonances observed in the ^{1}H NMR spectrum of $H_4SiW_{12}O_{40}/SiO_{2\text{-}(25)}$ (Figure S5, Supporting Information), adsorbed on fully hydroxylated and fully hydrated silica; this suggests that water has been produced during the reaction. Effectively, the total amount of $H_4SiW_{12}O_{40}/SiO_{2\text{-}(500)}$ protons significantly and progressively increases during the reaction with methane between 25 and 120 °C as indicated by the large increase in the overall integrated intensity of the ^{1}H MAS NMR spectra (see Figure 1 and Table S1, Supporting Information). These observations are consistent with the formation of water during the course of the methane reaction, which causes further hydration of the $H_4SiW_{12}O_{40}/SiO_{2\text{-}(500)}$ system. The signal at 5–6 ppm is indeed characteristic of water that is hydrogen bonded to silanols,[40] and the signals at 7–8 ppm can be attributed to HPA protons interacting with a hydrated silica surface, likely as $H_5O_2^+$.[41] The absence of autocorrelations in the DQ and TQ spectra is attributed to the high mobility of the species at 7–8 ppm, as evidenced by variable-temperature NMR experiments (Figure S6, Supporting Information) (as the temperature goes down below room temperature to −148 °C, this peak broadens and disappears).

Further evidence for the hydration of the HPA proton is obtained by following the reaction between $H_4SiW_{12}O_{40}/SiO_{2\text{-}(500)}$ and methane up to 120 °C by attenuated total reflectance (ATR) IR spectroscopy (860–1000 cm^{-1} range; Figure S7, Supporting Information): the band at 1006 cm^{-1} corresponding to the terminal W=O_d groups in Keggin-type HPA anions (Figure S8, Supporting Information), which are not involved in hydrogen bonding, decreases in intensity, and the band at 989 cm^{-1} corresponding to W=O_d···H···O_c shifts to 976 cm^{-1}.[42] This shift is consistent with the hydration of these groups, that is, the formation of the dioxonium ion $H_2O{\cdots}H^+{\cdots}OH_2$ that binds two Keggin units.[43,44] This is further supported by the change in the 2300–3500 cm^{-1} region of the IR spectrum associated with the vibrational modes of water (Figure S9, Supporting Information).[44]

The reaction between $H_4SiW_{12}O_{40}/SiO_{2\text{-}(500)}$ and methane thus produces both acetic acid and water on the surface. Water is not released from the solid below 190 °C. It remains bound and hydrates the initially dehydrated $H_4SiW_{12}O_{40}/SiO_{2\text{-}(500)}$ system. The intensity of the peaks at 7–8 ppm in the ^{1}H MAS solid-state NMR spectrum of $H_4SiW_{12}O_{40}/SiO_{2\text{-}(500)}$ in contact with methane at 120 °C indicates the following: (i) the water molecules produced interact with $H_4SiW_{12}O_{40}$ protons (only a weak residual signal at 3.3 ppm characteristic of pure hydrated silica (Figure S10, Supporting Information) is visible; it is known that 11–28 water molecules can typically be accommodated around Keggin units in hydrated $H_4SiW_{12}O_{40}$);[45] (ii) the hydrated $H_4SiW_{12}O_{40}$ protons are interacting with the silica surface (only a minor signal at ca. 9 ppm corresponding to unsupported hydrated $H_4SiW_{12}O_{40}$ (Figure S11, Supporting Information) is observed). Furthermore, by correlating NMR and GC data (Table S2, Supporting Information), the number of water molecules produced per molecule of CH_4 transformed into acetic acid or CO_2 below 350 °C can be estimated; it ranges from about one at 80 °C to about three at 120 °C. Hence, the stoichiometric equation can be written as follows:

$$2CH_4 + [H_2SiW_{12}O_{40}]^{2-}[{\equiv}Si{-}O(H)_2]^+_2 \rightarrow CH_3COOH + [H_2SiW_{12}O_{36}]^{2-}[H_3O]^+_2{\cdots}[{\equiv}Si{-}OH]_2$$

This implies partial reduction of the Keggin unit. This reduction was first verified by cyclic voltammetry (CV) carried

dx.doi.org/10.1021/ja309966j | J. Am. Chem. Soc. 2013, 135, 804–810

out on $H_4SiW_{12}O_{40}/SiO_{2\text{-}(500)}$ samples obtained before and after reaction with methane at 120 °C (Figure S12, Supporting Information). The sample before reaction exhibits four sets of well-defined, reversible, and repeatable voltammetric peaks, which means that, under the experimental conditions of cyclic voltammetry, consecutive redox transitions do not lead to any significant structural changes in $H_4SiW_{12}O_{40}$ supported on $SiO_{2\text{-}(500)}$. After reaction with methane at 120 °C, the marked changes in the cyclic voltammogram clearly show that the primary structure of $H_4SiW_{12}O_{40}$ in a $H_4SiW_{12}O_{40}/SiO_{2\text{-}(500)}$ sample is reorganized and that the $[W]^{VI}$ species has been reduced to lower valence.[46,47] The extent of the reduction was further estimated by X-ray photoelectron spectroscopy (XPS) measurements carried out on $H_4SiW_{12}O_{40}/SiO_{2\text{-}(500)}$ samples obtained after reaction with methane at 120 and 300 °C. The W 4f XPS spectrum recorded from $H_4SiW_{12}O_{40}/SiO_{2\text{-}(500)}$ (Figure S13A, Supporting Information) is composed of a spin−orbit doublet signal with binding energies for the W $4f^{7}_{/2}$ and W $4f^{5}_{/2}$ core levels of 36.6 and 38.4 eV, respectively. It is further fitted by two spin−orbit doublets. The major W $4f^{7}_{/2}$ component at 36.4 eV obtained after line fitting shows a similar binding energy value to that observed in pure bulk silicotungstic acid, which corresponds to individual Keggin units on the silica surface; the second component of lower intensity at 34.9 eV belongs to the $[W^{VI}]{=}O_d$ species in direct coordination with the silica surface.[48] After methane activation at 120 °C, the minor W $4f^{7}_{/2}$ component at 34.9 eV is shifted to a lower binding energy by 0.4 eV (to 34.5 eV) (Figure S13B, Supporting Information). With increasing temperature to 300 °C, this minor W $4f^{7}_{/2}$ component is further shifted to 33.6 eV (Figure S13C, Supporting Information). These results indicate that the tungsten species at the interface position is reduced to W^{IV} during methane activation.[49]

The role of the HPA−silica interface in the activation of methane (Figure 5) was confirmed by measuring the activity of four different $SiO_{2\text{-}(500)}$ supported HPA species (HPA = $H_4SiW_{12}O_{40}$, $H_3PW_{12}O_{40}$, $H_4SiMo_{12}O_{40}$, and $H_3PMo_{12}O_{40}$). The total amount of carbon-containing products (CH_3COOH and CO_2) released below 350 °C (Figure S15, Supporting Information) was observed to linearly correlate to the fraction of HPA acid protons that interact with the silica surface [$\equiv Si{-}O(H)_2]^+$ (Table S3, Figure S2(i), and Figure S14, Supporting Information). Interfacial protons appear key in achieving methane activation and functionalization; no such reactivity is observed over unsupported HPAs.

These data can be interpreted by an Olah-type superacidic mechanism in which hydrogen produced at low temperature (and absent from the gas phase below 120 °C) immediately reduces interfacial W^{VI} through a concerted mechanism generating water.[4,5] In such a mechanism, the proton interacting with both the terminal oxo ligand of HPA and the O of silanols could protonate the C−H bond of methane. The resulting H_2 molecule would reduce the oxo ligand of chemisorbed HPA.

It is only above 120 °C that one can observe by GC the gaseous hydrogen produced once the HPA has been reduced. At this stage, any further proposal relating to the detailed mechanism is speculative. We tentatively speculate that the carbonium CH_3^+ could react further with excess methane to give $C_2H_5^+$ plus hydrogen as described by Olah et al.[4,5] and more recently by Spivey et al.[50] This native hydrogen could

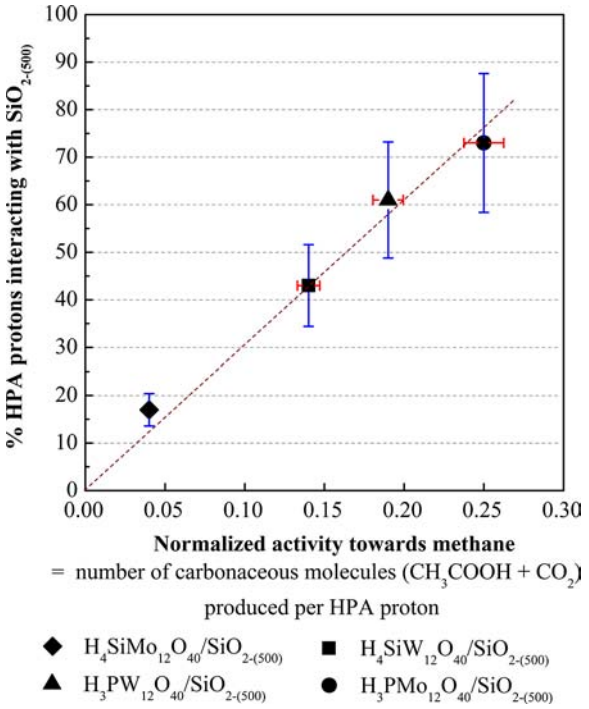

Figure 5. Correlation between the normalized amount of carbon-containing products (CH_3COOH and CO_2) produced below 350 °C in the gas phase upon reaction with CH_4 and the fraction of HPA protons interacting with the $SiO_{2\text{-}(500)}$ surface in HPA−$SiO_{2\text{-}(500)}$ samples. Rhombus, $H_4SiMo_{12}O_{40}$−$SiO_{2\text{-}(500)}$; square, $H_4SiW_{12}O_{40}$−$SiO_{2\text{-}(500)}$; triangle, $H_3PW_{12}O_{40}$−$SiO_{2\text{-}(500)}$; circle, $H_3PMo_{12}O_{40}$−$SiO_{2\text{-}(500)}$. Error bars are set at 20% vertically (values derived from ^1H NMR line fittings) and 5% horizontally (integration of CH_4-TPD signals in the 180−350 °C range).

reduce another $[H_2SiW_{12}O_{40}]^{2-}$ to $[H_2SiW_{12}O_{36}]^{2-}$ and water as in the previous steps. Once the $C_2H_5^+$ moiety is formed, acetic acid could easily be produced by reaction with the remaining tungsten oxo and water. In support of this, we found that ethane can also give acetic acid under identical conditions. We also considered that CO could react with the methyl cation to trap the acetyl derivative.[21] However, as yet even after careful studies, we have not observed any CO in the adsorbed or gas phase. Additionally, the possibility that residual acetonitrile could be hydrolyzed to acetic acid can be discounted, since it is not observed in the ^{13}C NMR spectrum of the unreacted material (Figure 1a) and so could not account for the subsequent large ^{13}C signals from acetic acid after reaction, which can thus only be due to the labeled methane yielding labeled acetic acid.

CONCLUSION

In conclusion, by chemisorbing four different dehydrated Keggin-type HPAs ($H_4SiW_{12}O_{40}$, $H_3PW_{12}O_{40}$, $H_4SiMo_{12}O_{40}$, and $H_3PMo_{12}O_{40}$) on a partially dehydroxylated $SiO_{2\text{-}(500)}$ surface via surface organometallic chemistry methods, we developed a bifunctional solid that can overcome the extreme conditions used in homogeneous systems and react with methane to produce acetic acid at room temperature and atmospheric pressure. Unlike other methane to acetic acid systems using Pd associated with sulfuric acid as the oxidant, no metal is present in our material; the chemistry is purely the result of the strong acidity, coupled with the redox capacity, of grafted HPA. Although the reaction is substoichiometric, it

dx.doi.org/10.1021/ja309966j | J. Am. Chem. Soc. 2013, 135, 804−810

sheds light on a simple and meaningful methane activation pathway over chemisorbed HPA. Since HPAs have the unique property of being reoxidized by oxygen/water,[51] we are now seeking methods to render the system catalytic.

EXPERIMENTAL SECTION

Starting Materials. Silicotungstic acid ($H_4SiW_{12}O_{40}\cdot xH_2O$), silicomolybdic acid ($H_4SiMo_{12}O_{40}\cdot xH_2O$), phosphotungstic acid ($H_3PW_{12}O_{40}\cdot xH_2O$), phosphomolybdic acid ($H_3PMo_{12}O_{40}\cdot xH_2O$), acetonitrile, and silica were purchased from Sigma–Aldrich. The four HPAs were used without further purification. Acetonitrile was dried and distilled prior to use. High purity gases (methane, 99.9995%; argon, 99.9999%) were purchased from Specialty Gases Center of Abdullah Hashim Industrial Gases & Equipment Co. Ltd. (Saudi Arabia) and dried prior to use.

Preparation of $SiO_{2\text{-}(500)}$. SiO_2 was compacted with distilled water, dried at 120 °C for at least 5 days, sieved, calcined at 500 °C in air for 4 h, and partially dehydroxylated at 500 °C for 12 h under high vacuum ($<10^{-5}$ mbar).

Preparation of HPA–$SiO_{2\text{-}(500)}$. HPA was dehydrated under high vacuum ($<10^{-5}$ mbar) at 100 °C for 1 h and then at 200 °C for 1 h. Most of the crystallization water was removed before solubilization of the HPA in dried acetonitrile and in contact with $SiO_{2\text{-}(500)}$. The mixture of dehydrated HPA dissolved in dry acetonitrile and $SiO_{2\text{-}(500)}$ was stirred at 25 °C for 12 h. The resulting HPA–$SiO_{2\text{-}(500)}$ powder was isolated after removal of the solution containing the unreacted HPA, dried under high vacuum ($<10^{-5}$ mbar), and then, stored under argon.

Dynamic Temperature-Programmed CH_4 Activation Reaction. The activation of methane was performed using a fixed-bed flow tubular reactor (stainless steel, internal diameter of 9 mm) operated at atmospheric pressure. A 250 mg sample was transferred into the reactor in a glovebox under argon and sealed off from air until dry methane was introduced. The reaction was started by introducing methane to the reactor at 25 °C and then finished at 500 °C after a temperature-programmed increasing process (temperature increase rate was 50 °C h^{-1}). During the whole temperature-programmed reaction, the methane flow rate was fixed at 5 mL min^{-1}. The products were analyzed by online Varian 490 micro-GC. All the lines and valves between the exit of the reactor and the micro-GC were heated to 120 °C to prevent the condensation of products. The separation and detection of gaseous products resulting from methane activation were carried out using Molsieve 5 Å, Pora Plot U, and CP-Sil 5CB columns and one TCD detector.

Characterizations. 1D ^1H MAS and ^{13}C CP/MAS solid-state NMR spectra were recorded on a Bruker AVANCE III-600 spectrometer operating at 600 and 150 MHz resonance frequencies for ^1H and ^{13}C, respectively, with a conventional double resonance 3.2 mm CPMAS probe. The spinning frequency was set to 17 and 10 kHz for MAS ^1H and ^{13}C experiments, respectively. NMR chemical shifts were reported with respect to TMS as an external reference. Additional details on solid-state NMR experiments are provided in the Supporting Information.

2D ^1H–^{13}C HETCOR solid-state NMR spectroscopy experiments were conducted on a Bruker AVANCE III-400 spectrometer using a 3.2 mm MAS probe. A total of 64 t_1 increments with 10 000 scans each were collected. The sample spinning frequency was 8.5 kHz, and the contact time for the cross-polarization step was set to 0.4 ms, which allowed the selective observation of the spatially close attached C–H pairs. Using longer contact times (5 ms), we found that it is possible to observe extra correlation peaks, which arise from longer-range dipolar interactions (e.g., to nonbonded protons). During acquisition, the proton decoupling field strength was also set to 75 kHz. Quadrature detection in ω_1 was achieved using the TPPI method.[52]

2D DQ and TQ homonuclear correlation MAS ^1H solid-state NMR spectra were acquired on a Bruker AVANCE III-800 or 500 MHz spectrometer with a conventional double resonance 3.2 mm CPMAS. One cycle of the standard back-to-back (BABA) recoupling sequence was used for the excitation and reconversion period.[53,54] The spectra were recorded in a rotor-synchronized fashion in t_1. Quadrature detection in ω_1 was achieved using the States–TPPI method.

ASSOCIATED CONTENT

Supporting Information

Additional experimental details including synthesis and characterization; NMR, IR, and XPS spectra; Keggin structure of α-$XM_{12}O_{40}^{x-}$ anion; cyclic voltammograms; plots of carbon-containing product evolution during temperature-programmed activation of methane on HPA–$SiO_{2\text{-}(500)}$; summary of amounts and types of protons in systems; and correlation between analyses of the GC and solid state. This material is available free of charge via the Internet at http://pubs.acs.org.

AUTHOR INFORMATION

Corresponding Author

jeanmarie.basset@kaust.edu.sa; valerie.caps@kaust.edu.sa; lyndon.emsley@ens-lyon.fr

Present Address

[⊥]Laboratoire des Matériaux, Surfaces et Procédés pour la Catalyse (LMSPC), UMR 7515 CNRS/ECPM/Université de Strasbourg, 25 rue Becquerel, 67087 Strasbourg Cedex 2, France. E-mail: caps@unistra.fr.

Notes

The authors declare no competing financial interest.

ACKNOWLEDGMENTS

The authors acknowledge KAUST Nuclear Magnetic Resonance Core Lab and technical assistance of Dr. Kazuo Yamauchi (NMR). The authors also wish to thank Dr. Aram Amassian, Mr. Ahmed E. Mansour, and Mr. Guy Olivier NGONGANG NDJAWA for their kind help in XPS measurements. M.S. acknowledges support from Dr. Xin Liu in HPA structure drawing. A.J.R. acknowledges support from an EU Marie-Curie IIF fellowship (PIIF-GA-2010-274574). This work was supported by funds from King Abdullah University of Science and Technology and SABIC (Saudi Basic Industries Corporation) company.

REFERENCES

(1) NaturalGas.org. Overview of Natural Gas. http://www.naturalgas.org/overview/background.asp (accessed Oct, 5, 2012.

(2) Hashiguchi, B. G.; Bischof, S. M.; Konnick, M. M.; Periana, R. A. *Acc. Chem. Res.* **2012**, *45*, 885.

(3) Crabtree, R. H. *Chem. Rev.* **1995**, *95*, 987.

(4) Olah, G. A.; Schlosberg, R. H. *J. Am. Chem. Soc.* **1968**, *90*, 2726.

(5) Olah, G. A.; Klopman, G.; Schlosberg, R. H. *J. Am. Chem. Soc.* **1969**, *91*, 3261.

(6) Goldberg, K. I.; Goldman, A. S. 223rd American Chemical Society Meeting, Orlando, FL, 2002.

(7) Shilov, A. E. *Activation of Saturated Hydrocarbons by Transition Metal Complexes*; Reidel, Dordrecht, The Netherlands, 1984.

(8) Periana, R. A.; Taube, D. J.; Evitt, E. R.; Loffler, D. G.; Wentrcek, P. R.; Voss, G.; Masuda, T. *Science* **1993**, *259*, 340.

(9) Periana, R. A.; Taube, D. J.; Gamble, S.; Taube, H.; Satoh, T.; Fujii, H. *Science* **1998**, *280*, 560.

(10) Stahl, S. S.; Labinger, J. A.; Bercaw, J. E. *Angew. Chem., Int. Ed.* **1998**, *37*, 2181.

(11) Levchenko, L. A.; Sadkov, A. P.; Lariontseva, N. V.; Koldasheva, E. M.; Shilova, A. K.; Shilov, A. E. *Dokl. Biochem. Biophys.* **2001**, *377*, 123.

(12) Labinger, J. A.; Bercaw, J. E. *Nature* **2002**, *417*, 507.

(13) Jones, C. J.; Taube, D.; Ziatdinov, V. R.; Periana, R. A.; Nielsen, R. J.; Oxgaard, J.; Goddard, W. A. *Angew. Chem., Int. Ed.* **2004**, *43*, 4626.
(14) Lersch, M.; Tilset, M. *Chem. Rev.* **2005**, *105*, 2471.
(15) Levchenko, L. A.; Lobanova, N. G.; Martynenko, V. M.; Sadkov, A. P.; Shestakov, A. F.; Shilova, A. K.; Shilov, A. E. *Dokl. Chem.* **2010**, *430*, 50.
(16) Periana, R. A.; Mironov, O.; Taube, D.; Bhalla, G.; Jones, C. J. *Science* **2003**, *301*, 814.
(17) Conley, B. L.; Tenn, W. J.; Young, K. J. H.; Ganesh, S. K.; Meier, S. K.; Ziatdinov, V. R.; Mironov, O.; Oxgaard, J.; Gonzales, J.; Goddard, W. A.; Periana, R. A. *J. Mol. Catal. A: Chem.* **2006**, *251*, 8.
(18) Xu, Z. T.; Oxgaard, J.; Goddard, W. A. *Organometallics* **2008**, *27*, 3770.
(19) Ahlquist, M.; Periana, R. A.; Goddard, W. A. *Chem. Commun.* **2009**, 2373.
(20) Bagno, A.; Bukala, J.; Olah, G. A. *J. Org. Chem.* **1990**, *55*, 4284.
(21) Hogeveen, H.; Lukas, J.; Roobeek, C. F. *J. Chem. Soc. D: Chem. Commun.* **1969**, 920.
(22) de Rege, P. J. E.; Gladysz, J. A.; Horvath, I. T. *Adv. Synth. Catal.* **2002**, *344*, 1059.
(23) Palkovits, R.; Antonietti, M.; Kuhn, P.; Thomas, A.; Schuth, F. *Angew. Chem., Int. Ed.* **2009**, *48*, 6909.
(24) Palkovits, R.; von Malotki, C.; Baumgarten, M.; Mullen, K.; Baltes, C.; Antonietti, M.; Kuhn, P.; Weber, J.; Thomas, A.; Schuth, F. *ChemSusChem* **2010**, *3*, 277.
(25) Forde, M. M.; Grazia, B. C.; Armstrong, R.; Jenkins, R. L.; Ab Rahim, M. H.; Carley, A. F.; Dimitratos, N.; Lopez-Sanchez, J. A.; Taylor, S. H.; McKeown, N. B.; Hutchings, G. J. *J. Catal.* **2012**, *290*, 177.
(26) Dobson, I. D. *Green Chem.* **2003**, *5*, G78.
(27) Fang, K. G.; Wang, X. P.; Zhang, J. L.; Cai, T. X. *Chin. Chem. Lett.* **2001**, *12*, 125.
(28) Sopa, A.; Waclaw-Held, A.; Grossy, M.; Pijanka, J.; Nowinska, K. *Appl. Catal., A* **2005**, *285*, 119.
(29) The starting material $H_4SiW_{12}O_{40}$−$SiO_{2\text{-}(500)}$ was prepared by the techniques used in surface organometallic chemistry. See the Supporting Information for details.
(30) Luzgin, M. V.; Rogov, V. A.; Kotsarenko, N. S.; Shmachkova, V. P.; Stepanov, A. G. *J. Phys. Chem. C* **2007**, *111*, 10624.
(31) Wang, X.; Qi, G.; Xu, J.; Li, B.; Wang, C.; Deng, F. *Angew. Chem., Int. Ed.* **2012**, *51*, 3850.
(32) Fulmer, G. R.; Miller, A. J. M.; Sherden, N. H.; Gottlieb, H. E.; Nudelman, A.; Stoltz, B. M.; Bercaw, J. E.; Goldberg, K. I. *Organometallics* **2010**, *29*, 2176.
(33) Legrand, A. P.; Hommel, H.; de la Caillerie, J. B. D. *Colloid. Surf. A* **1999**, *158*, 157.
(34) Grinenval, E.; Rozanska, X.; Baudouin, A.; Berrier, E.; Delbecq, F.; Sautet, P.; Basset, J. M.; Lefebvre, F. *J. Phys. Chem. C* **2010**, *114*, 19024.
(35) Kozhevnikov, I. V.; Sinnema, A.; Vanbekkum, H. *Catal. Lett.* **1995**, *34*, 213.
(36) DQ- and TQ-quantum proton spectroscopies under fast MAS have recently been shown to be powerful techniques to probe the structural and dynamic information inherent in proton−proton dipolar couplings. The DQ frequency in the ω_1 dimension corresponds to the sum of the two single quantum (SQ) frequencies of two coupled protons and correlates in the ω_2 dimension with the two individual ordinary proton frequencies. Similarly, the TQ frequency in the ω_1 dimension corresponds to the sum of the three SQ frequencies of three coupled protons and correlates in the ω_2 dimension with the three individual proton resonances. Three equivalent protons will thus give an autocorrelation peak along the $\omega_1 = 3\omega_2$ line of the 2D map. Conversely, groups of less than three equivalent spins will not give rise to diagonal signals in the spectrum.
(37) Geen, H.; Titman, J. J.; Gottwald, J.; Spiess, H. W. *Chem. Phys. Lett.* **1994**, *227*, 79.
(38) Rataboul, F.; Baudouin, A.; Thieuleux, C.; Veyre, L.; Coperet, C.; Thivolle-Cazat, J.; Basset, J. M.; Lesage, A.; Emsley, L. *J. Am. Chem. Soc.* **2004**, *126*, 12541.
(39) Avenier, P.; Taoufik, M.; Lesage, A.; Solans-Monfort, X.; Baudouin, A.; de Mallmann, A.; Veyre, L.; Basset, J. M.; Eisenstein, O.; Emsley, L.; Quadrelli, E. A. *Science* **2007**, *317*, 1056.
(40) Trebosc, J.; Wiench, J. W.; Huh, S.; Lin, V. S. Y.; Pruski, M. *J. Am. Chem. Soc.* **2005**, *127*, 3057.
(41) Ratcliffe, C. I.; Ripmeester, J. A.; Tse, J. S. *Chem. Phys. Lett.* **1985**, *120*, 427.
(42) Brown, G. M.; Noespirlet, M. R.; Busing, W. R.; Levy, H. A. *Acta Crystallogr., Sect. B* **1977**, *33*, 1038.
(43) Bielanski, A.; Datka, J.; Gil, B.; Malecka-Lubanska, A.; Micek-Ilnicka, A. *Catal. Lett.* **1999**, *57*, 61.
(44) Micek-Ilnicka, A. *J. Mol. Catal. A: Chem.* **2009**, *308*, 1.
(45) Izumi, Y.; Matsuo, K.; Urabe, K. *J. Mol. Catal.* **1983**, *18*, 299.
(46) Kulesza, P. J.; Faulkner, L. R.; Chen, J.; Klemperer, W. G. *J. Am. Chem. Soc.* **1991**, *113*, 379.
(47) Karwowska, B.; Kulesza, P. J. *Electroanalysis* **1995**, *7*, 1005.
(48) Berry, F. J.; Derrick, G. R.; Marco, J. F.; Mortimer, M. *Mater. Chem. Phys.* **2009**, *114*, 1000.
(49) Xie, F. Y.; Gong, L.; Liu, X.; Tao, Y. T.; Zhang, W. H.; Chen, S. H.; Meng, H.; Chen, J. *J. Electron Spectrosc. Relat. Phenom.* **2012**, *185*, 112.
(50) Vasireddy, S.; Ganguly, S.; Sauer, J.; Cook, W.; Spivey, J. J. *Chem Commun* **2011**, *47*, 785.
(51) Tungatarova, S. A. http://www.scientificfund.kz/index.php?option=com_content&view=article&id=22:structural.
(52) Marion, D.; Wuthrich, K. *Biochem. Biophys. Res. Commun.* **1983**, *113*, 967.
(53) Rataboul, F.; Baudouin, A.; Thieuleux, C.; Veyre, L.; Coperet, C.; Thivolle-Cazat, J.; Basset, J. M.; Lesage, A.; Emsley, L. *J. Am. Chem. Soc.* **2004**, *126*, 12541.
(54) Schnell, I.; Spiess, H. W. *J. Magn. Reson.* **2001**, *151*, 153.